

# Corrosion and thermal shock resistance of metal (Cu, Al) matrix composites reinforced by SiC particles

A. STROJNY-NĘDZA<sup>1\*</sup>, P. EGIZABAL<sup>2</sup>, K. PIETRZAK<sup>1</sup>, R. ZIELIŃSKI<sup>1</sup>, K. KASZYCA<sup>1</sup>,  
A. PIĄTKOWSKA<sup>1</sup>, and M. CHMIELEWSKI<sup>1</sup>

<sup>1</sup>Lukasiewicz – Institute of Electronic Materials Technology, ul. Wolczynska 133, 01-919 Warsaw, Poland

<sup>2</sup>Fundación Tecnalia Research & Innovation, Department of Foundry and Steelmaking,  
Mikeletegi Pasealekua 2, 20009 Donostia-San Sebastian, Spain

**Abstract.** This paper presents the results of studies concerning the production and characterization of Al-SiC/W and Cu-SiC/W composite materials with a 30% volume fraction of reinforcing phase particles as well as the influence of corrosion and thermal shocks on the properties of selected metal matrix composites. Spark plasma sintering method (SPS) was applied for the purpose of producing these materials. In order to avoid the decomposition of SiC surface, SiC powder was coated with a thin tungsten layer using plasma vapour deposition (PVD) method. The obtained results were analysed by the effect of the corrosion and thermal shocks on materials density, hardness, bending strength, tribological and thermal properties. Qualitative X-ray analysis and observation of microstructure of sample surfaces after corrosion tests and thermal shocks were also conducted. The use of PVD technique allows us to obtain an evenly distributed layer of titanium with a constant thickness of 1.5  $\mu\text{m}$ . It was found that adverse environmental conditions and increased temperature result in a change in the material behaviour in wear tests.

**Key words:** Metal-matrix composites, silicon carbide, wear resistance, corrosion, thermal shocks.

## 1. Introduction

Metal matrix composites have advantages over the conventional materials. In comparison to monolithic materials, MMCs have high strength-to-density and stiffness-to-density ratios, better fatigue resistance at room and elevated temperature [1, 2]. In addition, MMCs possess lower coefficients of thermal expansion (CTE) and better wear resistance in comparison to conventional materials. As a thermal management material, MMCs fully meet the requirement of high thermal conductivity, high thermal stability, high dimensional stability, low CTE and high processing temperature resistance [3]. Over the last few years MMCs have found many practical applications. They are used in production of engine parts, airplane fuselages, sensors, electronic packaging, etc. [4–6]. Depending on the future applications of the designed material, the key requirements are different, e.g. materials for use in the electronic industry should be characterized by the following properties: high thermal conductivity, thermal expansion coefficient adapted to the properties of semiconductors, good mechanical properties, ability to bond, stability of structure across heat cycles, and low fabrication cost [7]. Highly demanding specifications from the automotive and aerospace industry concerning fuel efficiency and emission standards on the one hand, and high standards concerning comfort and safety on the other hand, are the motivation for decreasing the weight of vehicles by using such com-

posites. The main development objectives are an increase in stiffness, wear resistance, as well as oxidation resistance at an elevated temperature [8, 9]. Aluminium (Al) and copper (Cu) reinforced by SiC are used in various applications due to their excellent thermo-physical properties such as low coefficient of thermal expansion, high thermal conductivity, and improved mechanical properties. Cu-SiC and Al-SiC composites enable high thermal and electrical conductivity and high toughness of metal matrix to be combined with high stiffness, hardness, and wear resistance of silicon carbide reinforcement [1]. The fact that such a combination of properties is possible makes these MMCs particularly interesting for wear applications. Examples include automobile brakes, cylinder bores and bearings of internal combustion engines. Al-MMCs reinforced with silicon carbide particles are chosen because of their low cost and low specific weight compared to other types of materials. One of the most important stages for producing MMCs by powder metallurgy is the sintering process. Among the various sintering methods, spark plasma sintering (SPS) technique is one of the most effective processes in consolidating materials [7–11]. Due to the fact that the generated heat in SPS process concentrates only on particle surface, grain growth is limited. When the electrical current flows, the whole system is heated via the Joule's effect. As a result, an increase in local temperature on grain-to-grain contact points is observed. This influences the speed of mass transport and the evaporation and convection processes. At the same time, oxides are removed from the surface of metal particles and the diffusion activation energy in the powder is decreased. This occurrence improves the densification of the material [12, 13]. It is possible to produce MMCs with planned properties by choosing the types and number

\*e-mail: agatastrojny@yahoo.pl

Manuscript submitted 2019-10-21, revised 2020-06-17, initially accepted for publication 2020-06-26, published in October 2020

of aluminium alloys and their reinforcement. In [14] it was reported that rife problems appearing during the fabricating of Al-SiC composites is the formation of  $Al_4C_3$  at the SiC/matrix interface as a result of interfacial reaction between Al and SiC ( $4Al + SiC = Al_4C_3 + 3Si$ ). The  $Al_4C_3$  phase is undesirable due to the fact that, apart from its fragility, it easily reacts with water vapor to form gaseous products that are responsible for the microcracking and, consequently, the destruction of materials ( $Al_4C_3 + 12H_2O \rightarrow 4Al(OH)_3 + 3CH_4\uparrow$ ). In order to protect SiC particles before the aggressive attack of liquid Al, barrier coatings ( $SiO_2$ ) are used or the amount of silicon in the matrix is increased [15]. A different situation takes place with molten Cu that decomposes SiC to Si and C at an elevated temperature [16]. According to [17], SiC decomposes in contact with Cu during the sintering process and due to this Si diffuses into the copper matrix and remaining carbon atoms form a layer. The solubility of Si in Cu is approximately 5at.% 850°C [18]. Additionally, carbon does not react with copper and, because of the low coefficient of friction, reduced strength of the interface is observed [19]. Therefore, special attention should be paid to the phenomena in the area of metal/ceramic interface. The consolidation process should assure the maximum densification of the material, but without any structural changes in the interface area. On the other hand, there are attempts to improve the properties of Cu/SiC interface by the introduction of an additional coating on reinforcement. Coating technique has been intensively studied for A-MMCs and Cu-MMCs. In addition, various properties of ceramics and metals, especially a large difference in the values of their coefficient of thermal expansion, adversely affect the quality of the bonding of the metal matrix and the reinforcement. In such a structure, thermal stresses may occur at the interface, which may result in a decrease in the material's mechanical properties. Only a good connection enables smooth transfer of, e.g. heat flux or stress from the matrix to the reinforcing phase, and thus obtaining very good mechanical and functional properties of the composites. To achieve this, the surface of ceramic reinforcement must be protected. Recently, we have demonstrated that the use of Cr, W, Mo as coatings improves the structure and properties of metal/ceramic interfaces [16].

This work reports the results of the examination of structure and properties of Cu-SiC and Al-SiC composite materials, containing silicon carbide particles, coated with a thin tungsten layer by plasma vapour deposition technique.

For application in the automotive industry, the thermal and mechanical properties of the materials were determined after their exposure to a corrosive environment and to variable heat loads. The effects of corrosion and thermal shock tests on the material density, hardness, bending strength, tribological and thermal properties were analysed.

## 2. Experimental procedure

In this work, copper powder produced by NewMet Koch, with a grain size of 40  $\mu m$ , purity of 99.99% (Fig. 1a) and aluminium powder product by Goodfellow with a grain size <60  $\mu m$ ,

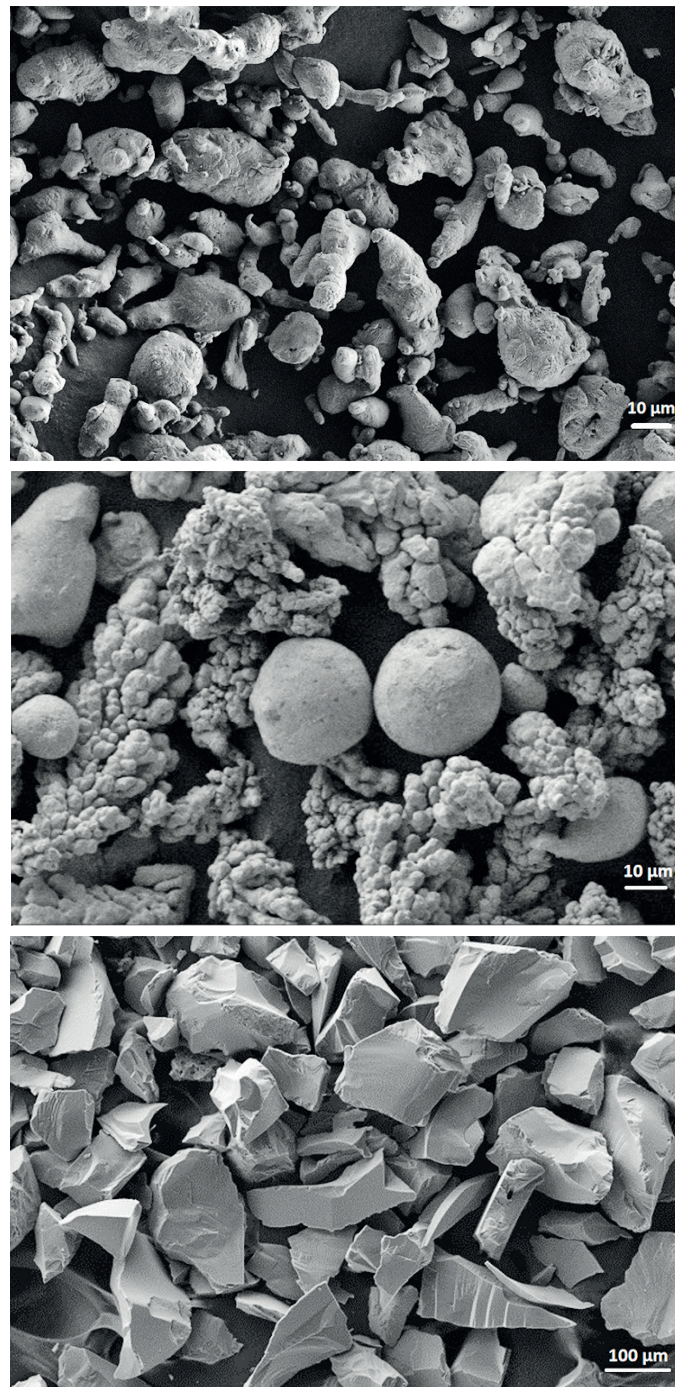


Fig. 1. Morphology of starting materials: a) Al, b) Cu and c) SiC

purity of 99.99% (Fig. 1b) were used as the matrix starting materials. Silicon carbide particles (Fig. 1c) with a mean size between 40–80  $\mu m$  (Fig. 2a) (product of Saint Gobin) and purity 99.99% were selected as the reinforcement. The SEM image of SiC powder particles (Fig. 1c) distinguishes two general types of particles. The first group of particles having full 3D symmetry, i.e.  $DX \sim DY \sim DZ$ , and those that have 2D symmetry, type  $DX \sim DY \gg DZ$ , (flattened particles). X-ray analysis of SiC powders (Fig. 2) showed that it is a material consisting of 88vol.% SiC 6H and 12vol.% SiC 15R.

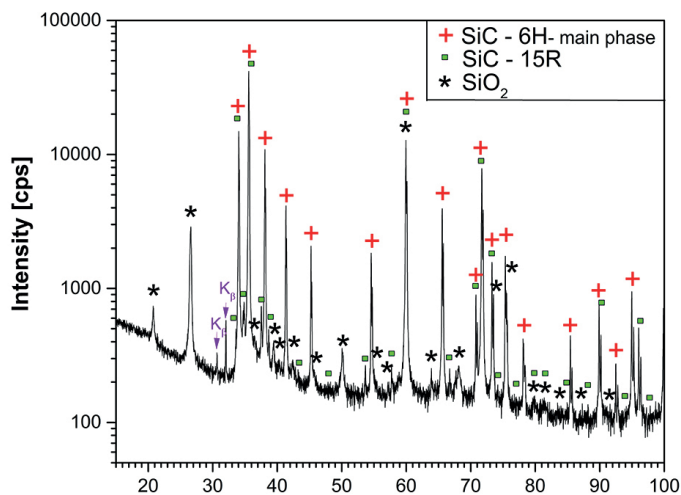


Fig. 2. X-ray analysis of SiC powder

To protect SiC particles against decomposition they were covered with a tungsten layer of 1.5  $\mu\text{m}$  thickness using plasma vapour deposition method (PVD). In order to ensure a uniform powder coating, a special spot for powder mixing in vacuum chamber was set up. The process of spraying was conducted in ULVAC sputtering system (Figs. 3a, 3b). The process was conducted for 12 h at the power of 200 W emitted by the installation's high-frequency generator. The morphology of the silicon carbide coated by tungsten is shown in Fig. 3c.

Powder mixture with 30vol.%SiC/W particles with aluminium and copper matrices were prepared using a planetary ball mill (Pulverisette 6, Fritsch GmbH, Germany). The mixing process was conducted for 4 h at a rotational speed of 200 rpm in argon atmosphere, using a vial (250 ml) and balls ( $\varnothing = 10$  mm) both made of WC/Co while 2 wt.% of stearic acid was added

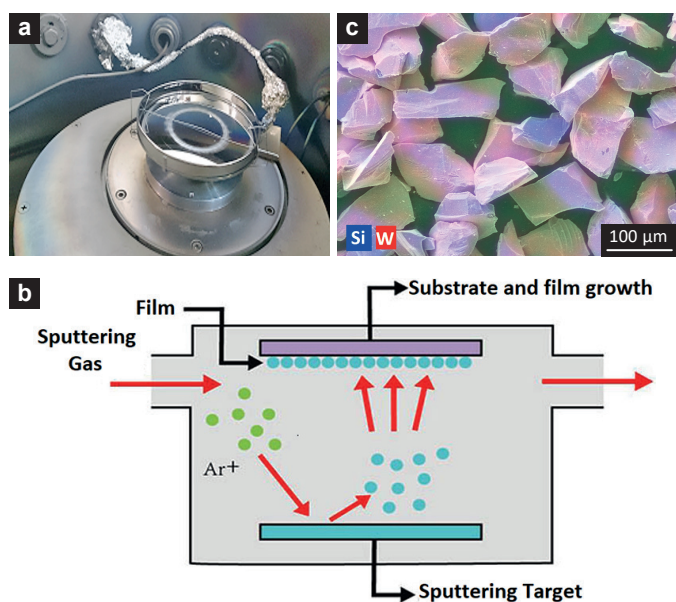


Fig. 3. Sputtering system: a) equipment, b) scheme and c) morphology of the SiC particles coated by tungsten

as a process control agent. The densification of the powder mixtures of Cu-30%SiC/W and Al-30%SiC/W was conducted using spark plasma sintering method. SPS densification process was performed in a vacuum chamber ( $5.0 \times 10^{-5}$  mbar) under the following conditions: sintering temperature 950°C for Cu-MMC and 590°C for Al-MMC, heating rate – 100°C/min, holding time – 10 mins, and pressure – 20 MPa.

Corrosion resistance tests in a salt chamber (environment: 50 g/l NaCl, temperature 35°C, total time 96 hours) were performed. Every 24 hours photos of the samples were taken (Fig. 4).

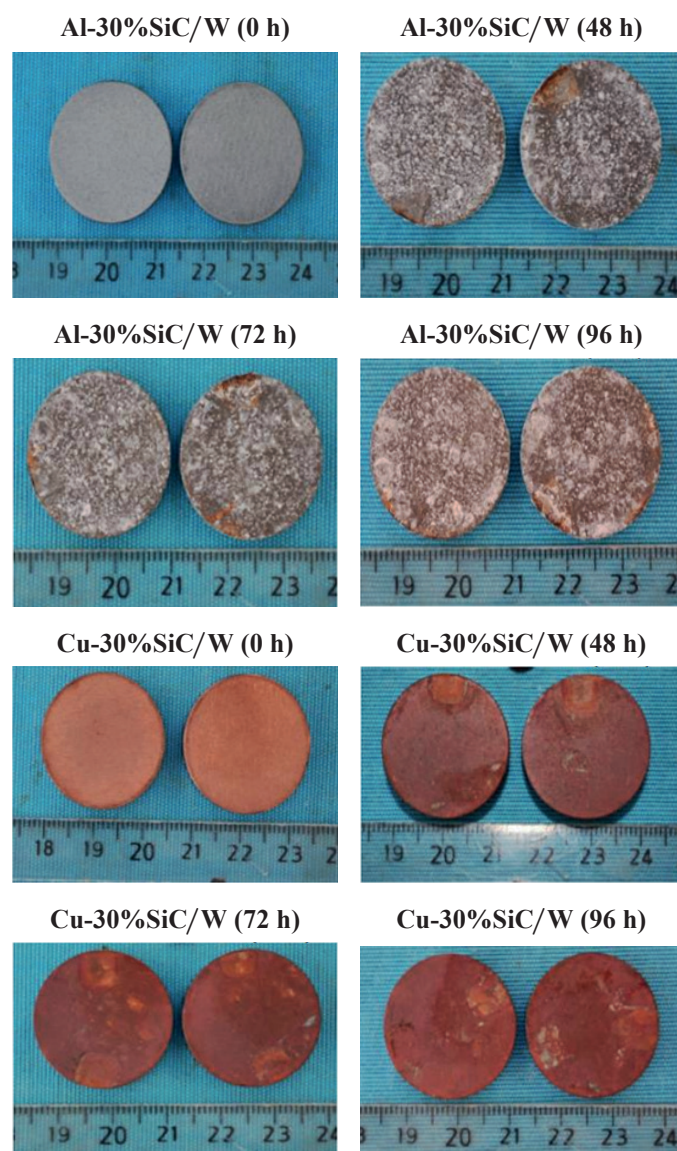


Fig. 4. Composites samples before, during and after corrosion tests

The developed MMCs were subjected to resistance tests for cyclic temperature changes using the testing system presented in Fig. 5. The tests were conducted in the heating-cooling regime, using a maximum temperature of 400°C for Al-SiC/W and 600°C for Cu-SiC/W composites. Changes in

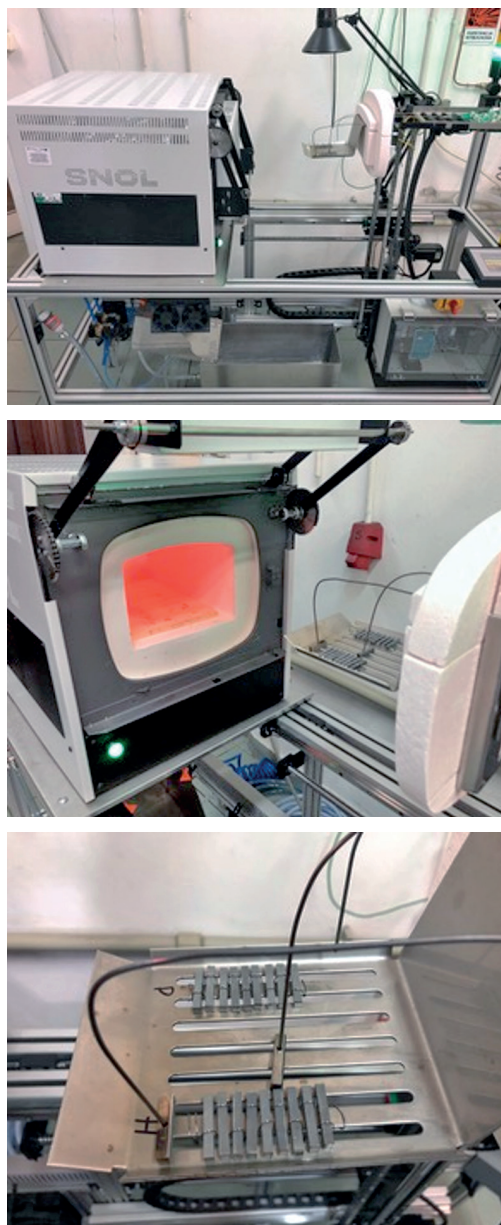


Fig. 5. System for testing resistance to cyclic temperature changes

the materials structure, density, hardness, bending strength and thermal properties after 500 cycles of heating-cooling cycles were analyzed.

The tribological tests were done using high temperature tribotester from Anton Paar company. The tests were performed at two temperatures: RT and 100°C. In the test Al<sub>2</sub>O<sub>3</sub> balls with 6 mm diameter and force 10 N were applied. As a protective atmosphere, argon was used. Tribological properties were tested on composite samples that previously had been subjected to corrosive and thermal shocks tests. Composite samples that were not exposed to adverse chemical and thermal factors were used as the reference material. The density of the obtained composite materials was measured by the hydrostatic method. The microstructures of the materials were examined via scanning electron microscopy (SEM) using AURIGA CrossBeam-

Workstation. The hardness (HV3) was tested with a Vickers diamond indenter using a load of 29 N with a loading time of 10 s. Each indentation was placed at least 10 diagonal lengths away from the adjacent indentation. The hardness results were averaged over 10 indentations per specimen. The bending strength was examined in a ZWICK 1446 strength machine. The samples intended for the bending strength tests had a size of 15×1×1 mm, and the head load was 10 kN. The thermal conductivity  $\lambda$  of the composites was measured using the Laser Flash Analyser LFA457/Netzsch. The  $\lambda$  measurement principle was as follows. The front side of a plane parallel solid sample is heated by a short laser pulse (Nd-YAG). The heat induced propagates through the sample and causes a temperature increase on the rear surface. The increase in temperature is measured versus time by using an infrared detector. The thermal diffusivity ( $a$ ) and, in most cases, the specific heat ( $c_p$ ) can be ascertained using the measured signal. If the density ( $\rho$ ) and the specific heat are known, the thermal conductivity ( $\lambda$ ) is determined from the relation (1):

$$\lambda = C_p \cdot \rho \cdot a, \quad (1)$$

where:  $\lambda$  – thermal conductivity in W/mK,  $\rho$  – density in g/cm<sup>3</sup>,  $c_p$  – specific heat in J/g K,  $a$  – thermal diffusivity in mm<sup>2</sup>/s [20]. In order to determine the value of heat conductivity, specific heat values were assumed on the basis of the mixing rule.

Qualitative phase analysis of the materials after corrosion tests (Cu-30SiC/W and Al-30SiC/W) was performed by means of powder X-ray diffraction (XRD) method. Polycrystalline materials in the form of bulk specimens (non-powdered) were studied. The experiments were performed using a universal Rigaku SmartLab 3 kW X-ray diffractometer equipped with a Cu X-ray tube and a 1D high-speed silicon semiconductor strip detector (D/teX Ultra 250). Powder diffraction patterns were measured in the reflection Bragg-Brentano geometry ( $\theta/2\theta$  scan) and the continuous scanning mode was used. Furthermore, in the case of Al-30SiC/W, parallel geometry with grazing incidence of primary beam was also applied to suppress strong substrate signals. Qualitative phase analysis was performed using a PDF4+2019 database and PDXL2 Software supplied by Rigaku.

### 3. Results and discussion

Figure 6 represents the microstructure of Al-30SiC/W and Cu-30SiC/W composite materials obtained by SPS technique. Microstructural analysis of sintered composites using scanning microscopy focused on the assessment of the quality of bonding between ceramic grains and the metal matrix as well as the quality of the materials, i.e. the distribution of the reinforcing phase and absence of any structural defects and porosity, which could have a significant negative influence on mechanical and thermal properties of the composites. As it can be seen in these figures, SiC particles had relatively strong bonding with aluminium and copper matrices and it is apparent that the sintering temperature and sintering time in SPS method were good.

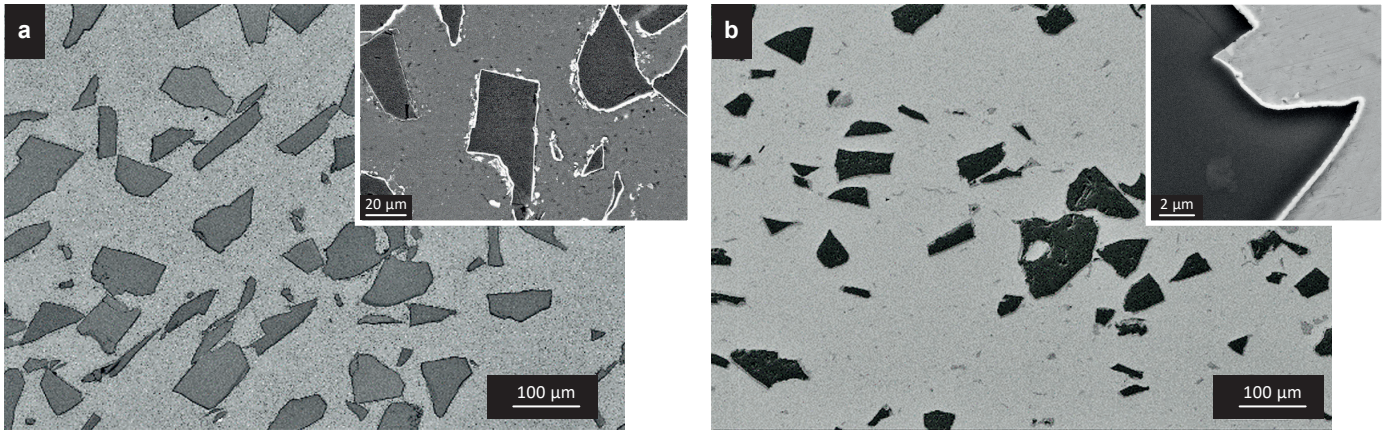


Fig. 6. SEM images of a) Al-30SiC/W and b) Cu-30SiC/W composites

One of the most important issues in manufacturing metal matrix composites by powder metallurgy techniques is to get a good bonding of metal particles with reinforcement and to form uniform metal/ceramic interfaces [21]. Figure 7 shows the interface between SiC particles (covered by W) with the aluminium matrix, where strong bonding without any discontinuities was observed. Particular grains are well separated from one another and no SiC aggregates can be found. The average thickness of the tungsten layer was estimated to be 1.5 μm.

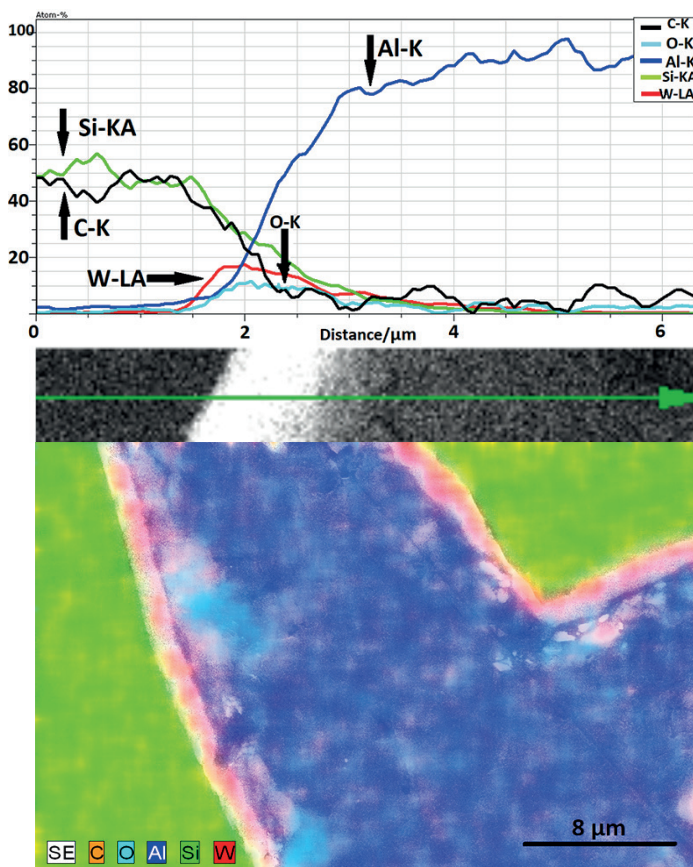


Fig. 7. Linear (left) and surface (right) distribution of elements (Al, Si, C, W, O) across the metal/ceramic interface of Al-SiC/W composite

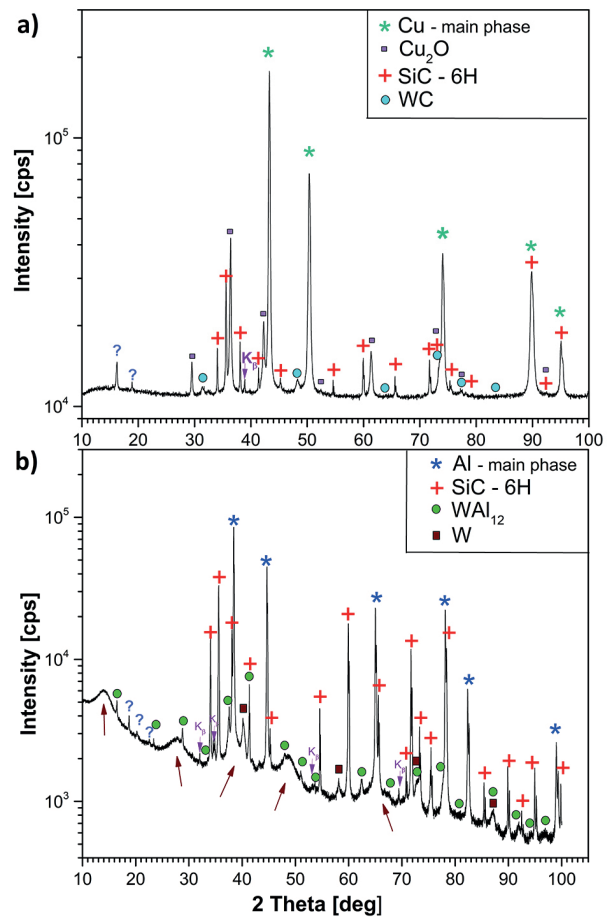


Fig. 8. Diffraction patterns of a) Cu-30SiC/W and b) Al-30SiC/W composites

Composite samples after corrosion tests were subjected to X-ray diffraction tests to analyze the surface composition. Qualitative phase analysis of the Cu-30SiC/W sample indicated dominant presence of Cu phase. Silicon carbide (6H-SiC), copper oxide  $\text{Cu}_2\text{O}$  (cuprite) and a trace amount of a less crystallized tungsten carbide (WC) phase were also observed. An experimental diffraction pattern with reference lines of matching phases from a database is presented in Fig. 8. The high

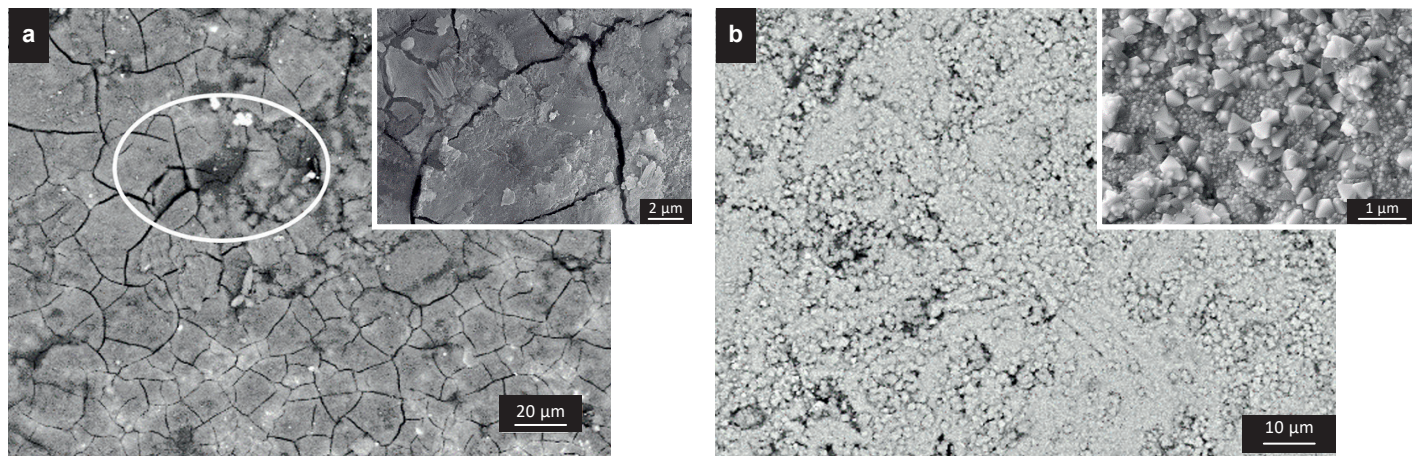


Fig. 9. SEM photos of surface of a) Al-30SiC/W and b) Cu-30SiC/W composites after corrosion test

background of experimental diffraction pattern is associated with a Cu fluorescence effect. Qualitative phase analysis of the Al-30SiC/W sample indicated the presence of aluminium (Al), silicon carbide (6H-SiC), tungsten (W),  $WAl_{12}$  intermetallic phase and a trace amount of an unidentified phase. The unresolved wide lines indicate the presence of an amorphous phase, which may be related to the oxidation process. The experimental diffraction pattern with reference lines of matching phases from a database is presented in Fig. 8.

The results of density measurements are presented in Table 1. The theoretical density of the composites were defined for the assumed volume contents, using the density of copper

$\rho_{Cu} = 8.89 \text{ g/cm}^3$ , aluminium  $\rho_{Al} = 2.71 \text{ g/cm}^3$  and silicon carbide  $\rho_{SiC} = 3.20 \text{ g/cm}^3$ .

Application of SPS technique allowed to obtain a material with a high relative density of 97–99%. The resulting composites were characterized by a negligible porosity, which is also confirmed by the observation of their microstructure. Measurements of the density of composite materials that have been subjected to corrosion and thermal shocks showed a slight change in this value. For samples after corrosion tests, a decrease in density was observed. The decrease of density after corrosion tests is attributed to the changes in the surface microstructure of the composite, microcracks formation and loss of consistency of the corroded layer with the materials. Figure 9 shows the surface of the Al-30SiC/W composite after exposure to NaCl solution. Generally, it has been found that the Al-SiC composites showed better corrosion resistance when compared with pure Al matrix, which has been confirmed in [22]. It may be attributed to the fact that SiC particles remain inert in the NaCl solution. The surface analysis of elements showed that after a corrosion test on the surface of the samples, a thin layer was formed, which included such elements as Na and Cl in both examined cases. This layer is characterized by discontinuity and numerous cracks that have affected the density of this material. Figure 9a shows a SEM micrograph of Al-30SiC/W composite where preferential localized corrosion can be seen and where corrosion starts in the interior of the sample and later expands to the surface. Figure 9a shows the paths where corrosion progresses on corroded surface of composite, here SiC particles are partially detached at pits, which are present at SiC/matrix interface. Fabrication of metal-ceramic composites sometimes leads to the formation of new components on the interface between the matrix and reinforcements, which can also influence corrosion. For example, it has been reported [23] that  $Al_4C_3$  reaction product can be formed at the SiC particles/matrix interface during the fabrication of Al-SiC composites, which can result in a severe loss of corrosion resistance. Some investigators have concluded that the increased corrosion rate is due to the formation of  $Al_4C_3$  at the interface [24]. Figure 9a shows that the surface of the samples underwent severe degradation,

Table 1

Results of density, hardness and bending strength measurements of pure aluminium, pure copper, and composite materials.

Material type		Measured density (g/cm <sup>3</sup> )	Relative density (%)	Hardness HV3	Bending strength (MPa)
Al	–	2.68	99.26	35	–
Al-SiC/W	–	2.82	99.05	61	154
	after corrosion	2.79	98.18	64	168
	after thermal shocks	2.83	99.29	78	173
Cu	–	8.86	99.66	55	–
Cu-SiC/W	–	7.03	97.80	108	174
	after corrosion	6.90	96.03	106	183
	after thermal shocks	7.17	99.81	125	201

especially along the grain boundaries. These grain boundaries provide preferential corrosion initiation sites because of the discontinuity in the surface due to the change in structure. Corrosion progresses leading to an intense porous structure near the interface. Surface analysis of elements (EDX) confirmed that a layer consisting of Na, Cl as well as NaCl salt crystals was formed on the surface of the composite materials. The resulting NaCl crystals appeared on the surface of Cu-30SiC/W as well, as shown in Fig. 9b. Copper has long been employed in many applications because of its good mechanical properties and corrosion resistance. In some highly aggressive environments copper still suffers from serious damage. For instance, in an aerated chloride medium, the corrosion of copper occurs at a noticeable rate.

Very high concentration of Cl ions results in the formation of electrolyte layer on the Cu surface. Moreover, this layer serves as a barrier against low aggressive media; this phenomenon is called the self-protective effect [25]. NaCl crystalline grows in a homogeneous manner on differently oriented single-crystal Cu surfaces [26]. Deposition on NaCl islands of different height are found on Cu, mainly single islands are present (Fig. 9b). The corrosion behaviour of copper under chloride-containing ions involves the formation of a protective layer consisting of  $\text{Cu}_2\text{O}$  formed as a result of rapid diffusion of oxygen. The  $\text{Cu}_2\text{O}$  layer, which is a p-type semiconductor and thus has low electrical conductivity, is mainly responsible for the high resistance [27, 28]. After a long immersion time, the protective  $\text{Cu}_2\text{O}$  layer suffered various degrees of attack and can be converted into  $\text{Cu}_2(\text{OH})_3\text{Cl}$  and  $\text{Cu}_2(\text{OH})_2\text{CO}_3$  in the presence of chloride ions. This happens after a very long period of copper exposure to a corrosive environment.

For samples that were subjected to thermal shocks, small increase in density was observed. A long process of heating materials can contribute to the further densification of the material due to the diffusion processes. Some materials obtained by techniques such as hot pressing or hot isostatic pressure are usually subjected to an additional thermal process to improve the density of these materials. As a result of reheating the material, grain growth and individual pores elimination can be observed.

Table 1 presents the results of Vickers hardness measurements. The particulate reinforcements such as SiC are generally preferred to impart higher hardness.

The coating of reinforcements with W also leads to good quality of interface characteristics and hence contributes to improving hardness. In [29] it was observed that interface discontinuities in Cu-SiC composites (SiC grains not covered with a protective layer) affected the deterioration of mechanical properties.

When 30vol.% SiC is introduced into aluminium and copper matrices, twofold increase in hardness value was observed in relation to pure Al and Cu sinters. Moreover, higher hardness values were indicated for both composite materials that were subjected to thermal shocks. In both cases, a thin layer of metal oxides appeared on the surface of the thermally explored materials (Fig. 10). It should be mentioned that thermal shock tests were conducted in the water environment and in the air

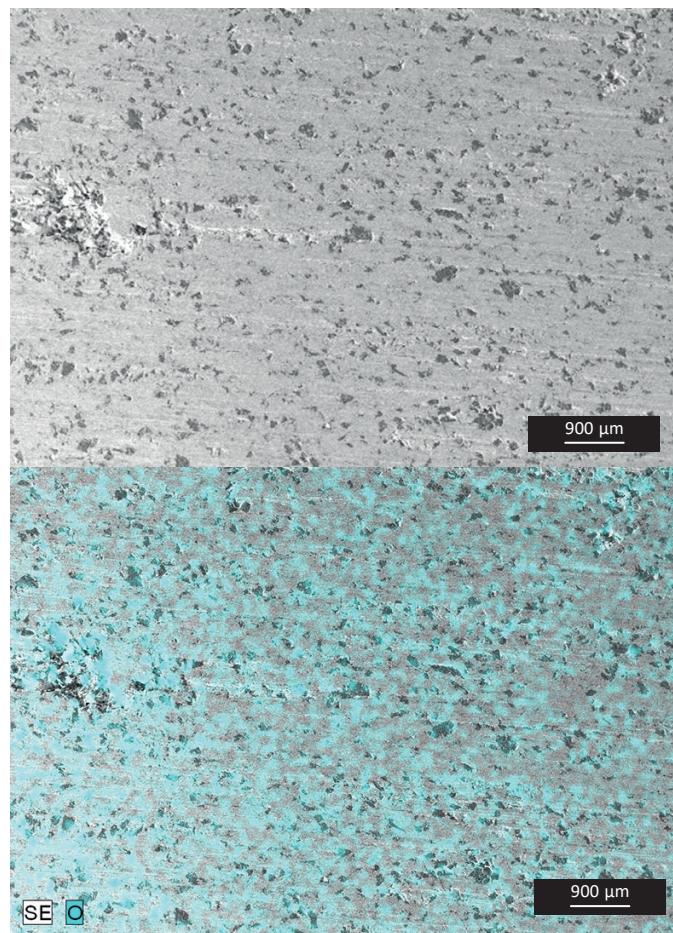


Fig. 10. SEM/EDX surface analysis of elements of Cu-30SiC/W composite after thermal shocks

at elevated temperatures. This, for sure, facilitates the formation of surface oxides and leads to surface strengthening of the material.

Hardness measurements of composites after the corrosion test indicate a slight increase in the hardness value in relation to the starting materials. As shown above, as a result of chemical interactions, oxides of higher hardness than the matrix material are formed on the surface of the composite. At the same time, numerous microcracks are created in the structure of the surface layer, which reduces the material's ability to transfer mechanical loads. Therefore, the effect of strengthening and weakening cancel each other out and the hardness is rather stable.

It was observed that bending strength increased with the growing hardness of the samples (Table 1). The effect of increase in the mechanical strength of composites can be related with the densification of the material. The decrease of pores and other discontinuities in the materials structure leads to improvement of bending strength.

Table 2 presents the results of the coefficient of friction and the depth of the groove formed during tribological tests for all analyzed composites. The comparison of friction coefficient changes vs. time for RT and 100°C of two groups of materials under investigation is presented in Figs. 11, 12.

Table 2

The results of wear resistance; coefficient of friction ( $\mu$ ) and groove depth of obtained composites

Material type		Tribological test at RT		Tribological test at 100°C	
		$\mu$	groove depth [ $\mu\text{m}$ ]	$\mu$	groove depth [ $\mu\text{m}$ ]
Al-3SiC/W	–	0.65	142	0.60	153
	after corrosion	0.50	109	0.48	145
	after thermal shocks	0.70	93	0.65	110
Cu-3SiC/W	–	0.50	64	0.55	58
	after corrosion	0.55	57	0.45	45
	after thermal shocks	0.70	41	0.65	39

Figure 11 shows the changes in coefficient of friction in terms of the time under the loads of 10 N for composite materials after corrosion tests. As it can be seen, the temperature growth during the wear process reduces the friction coefficient in all cases analyzed. The highest values of friction coefficient were recorded for samples after thermal shock tests. These

composites were characterized by the highest value of hardness and along with the increase in hardness, the resistance to movement increases, and thus the friction coefficient increases. The raise in the coefficient of friction can be attributed to the oxide layer formed during thermal shock tests in air on the surface of the samples. In this case, the volume of the groove depth was the minimum.

A more stable course of wear was observed at room temperature than that at elevated temperature. The general wear mechanism is similar for all materials. This is abrasive wear based on plastic deformation. The tribofilm formed on the surface of composite materials after corrosion tests is unstable and does not significantly affect the wear process. With such a heavy load, the counter-body is worn to create additional wear products. During wear tests in Cu-SiC/W composites, numerous micro cracks were observed in the friction area.

Representative images of the groove area are presented in Figs. 12, 13. The microstructure of the groove for Al-30SiC/W composite is very inhomogeneous: gaps, chipping and accretion are present, which cause rapid friction. For Cu-30SiC/W composites, the surface of the grooves is relatively smooth.

There was a plastic deformation/abrasion consisting in covering the ceramic phase with plastic copper. Slip lines are visible along which the counter-body had travelled. Individual breakouts are well-distinguished in the structure. No visible loose wear products that are pressed into the groove surface during the process.

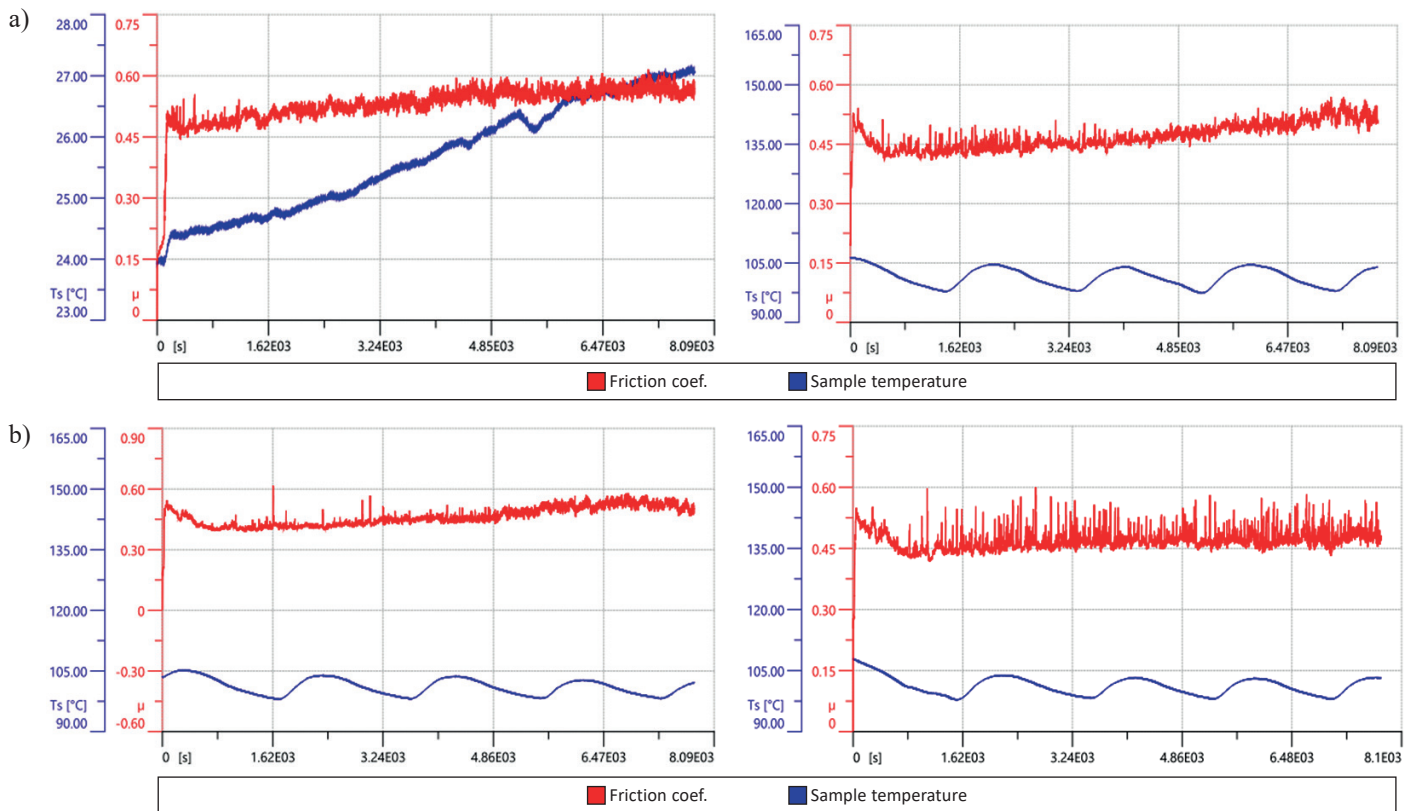


Fig. 11. Changes of the friction coefficient for two temperatures: (RT, 100°C) for: a) Al-30SiC/W and b) Cu-30SiC/W after corrosion tests



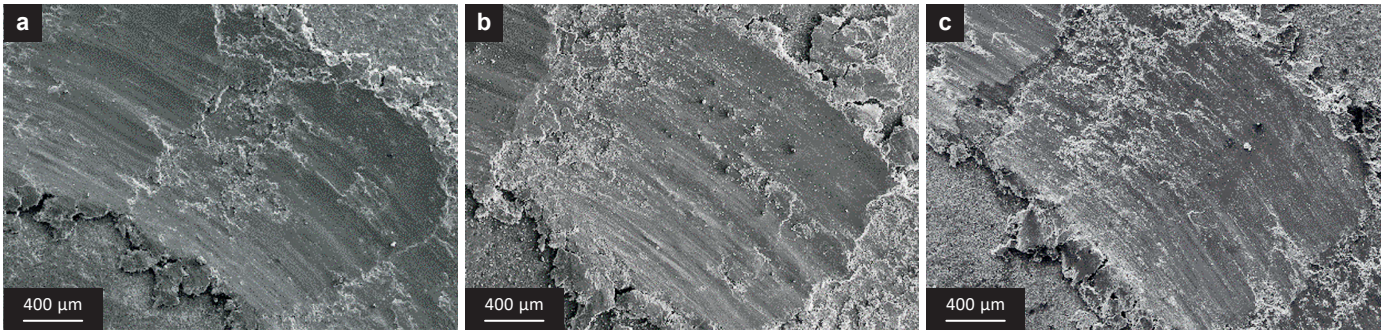


Fig. 12. SEM images of the groove area for: a) Al-30SiC/W, b) Al-30SiC/W after corrosion and c) Al-30SiC/W after thermal shock tests

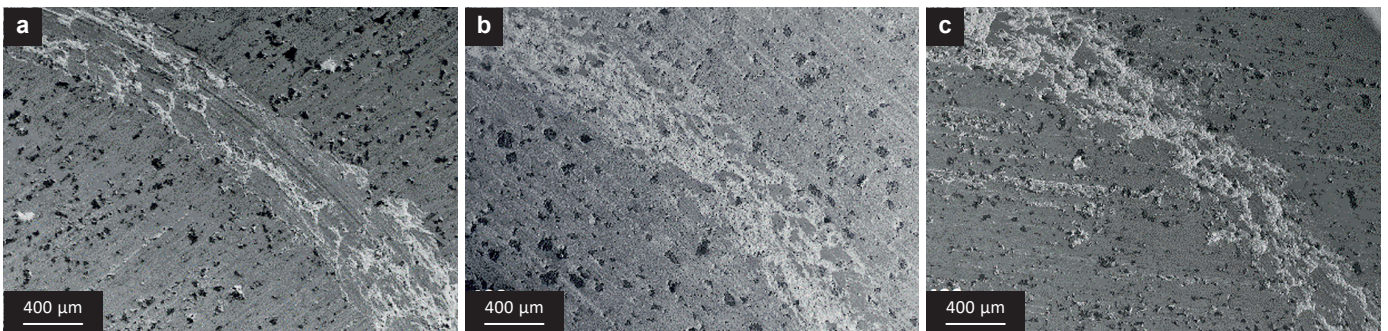


Fig. 13. SEM images of the groove area for: a) Cu-30SiC/W, b) Cu-30SiC/W after corrosion and c) Cu-30SiC/W after thermal shock tests

Thermal conductivity of Cu-30SiC/W and Al-30SiC/W composite materials, derived from the measurements of thermal diffusivity, are presented in graphical form in Figs. 14, 15. The graphs show the changes in conductivity as a function of the temperature measured. The highest value corresponds to the material that had not been subjected to adverse environmental conditions (corrosion, elevated temperature). The same behaviour was observed for Cu-MMCs. Metal oxides absorbed on the surface of these materials affect the reduction of thermal conductivity.

#### 4. Conclusions

In this study, the influence of corrosion and thermal shock tests on the microstructure, thermal and mechanical properties of Cu and Al based composites was investigated. Because of a high reactivity of Cu-SiC and Al-SiC systems at an elevated temperature, it seems purposeful to cover the SiC powder with a protective metallic layer. Based on the results presented, the following conclusions can be drawn. By SPS technique, composites based on copper and aluminium and containing SiC reinforcement can be successfully obtained. There was no sensible sign of microcracks or porosity in both composites and strong bonding was achieved at the metal/ceramic interfaces. Owing to PVD technique, it was possible to obtain a thin and discontinuities-free tungsten coating (1.5 μm) on SiC grains. The use of this layer prevents silicon carbide from decompos-

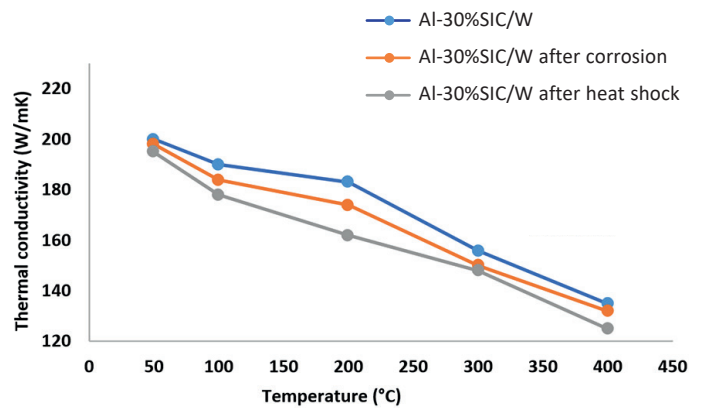


Fig. 14. Thermal conductivity vs temperature for: Al-30SiC/W

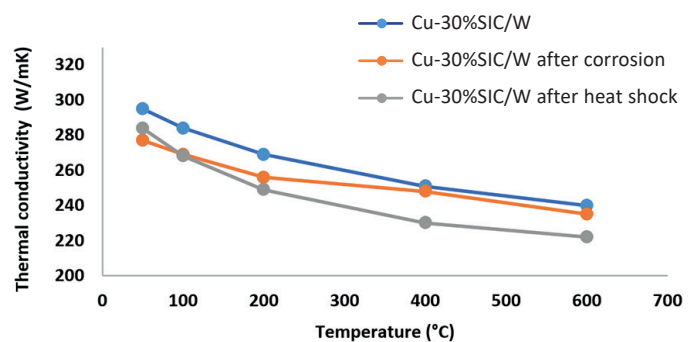


Fig. 15. Thermal conductivity vs temperature for Cu-30SiC/W

ing. The increase of material hardness was obtained after thermocycling tests. The oxidation of Cu-SiC and Al-SiC composites resulted in surface chemical changes. The new oxide phase was detected, which results in the increase in hardness, flexural strength, and improved wear resistance. The obtained composites are characterized by good corrosion resistance, variable heat load as well as good thermal properties and high frictional wear resistance. The adverse environmental conditions and elevated temperature result in a decrease in the thermal conductivity of the tested composites. Therefore, they can be used as wear resistance materials in automotive and aerospace industries.

**Acknowledgements.** This work was supported by the KMM-VIN Mobility Research Fellowship Program [Grant in the 10th Call].

## REFERENCES

- [1] G.B. Veeresh Kumar, C.S. Rao and N. Selvaraj, “Mechanical and tribological behavior of particulate reinforced aluminium metal matrix composites – a review”, *J Min & Mater Char & Eng.* 10, 59–91 (2011).
- [2] G.F. Celebi Efe, I. Altinsoy, M. Ipek, S. Zeytin and C. Bindal, “Some properties of Cu-SiC composites produced by powder metallurgy method”, *Kovove Mater.* 49, 131–136 (2011).
- [3] S. Bathula, R.C. Anandani, A. Dhar and A.K. Srivastava, “Microstructural features and mechanical properties of Al5083/SiC metal matrix nanocomposites produced by high energy ball milling and spark plasma sintering”, *Mater. Sci. Eng. A.* 545, 97–102 (2012).
- [4] A. Leifert et al., “Mechanical reinforcement of copper films with ceramic nanoparticles”, in *Dev. Strateg. Mater. Compu. Des.* V. 361–366 (2015).
- [5] E. Hong, B. Kaplin, T. You, M.S. Suh, Y.S. Kim and H. Choe, “Tribological properties of copper alloy-based composites reinforced with tungsten carbide particles”, *Wear* 270, 591–597 (2011).
- [6] K.K. Deng et al., “Microstructure and strengthening mechanism of bimodal size particle reinforced magnesium matrix composite”, *Compos. Part A-Appl. Sci. Manuf.* 43, 1280–1284 (2012).
- [7] M. Chmielewski, K. Pietrzak, A. Strojny-Nędzka, D. Jarzabek and S. Nosewicz, “Investigations of interface properties in copper-silicon carbide composites”, *Arch. Metall. Mater.* 62, 1315–1318 (2017).
- [8] V. Rajković, D. Bozić, M. Popović and M.T. Jovanović, “The influence of powder particle size on properties of Cu-Al<sub>2</sub>O<sub>3</sub> composites”, *Sci. Sinter.* 41, 185–192 (2009).
- [9] M. Shabana, B.L. Karihaloo, H.X. Zhu and S. Kulasegaram, “Influence of processing defects on the measured properties of Cu-Al<sub>2</sub>O<sub>3</sub> composites: A forensic investigation”, *Compo.:Part A.* 46, 140–146 (2013).
- [10] A. Pakdel, A. Witecka, G. Rydzek and D.N. Awang Shir, “A comprehensive microstructural analysis of Al-WC micro- and nano-composites prepared by spark plasma sintering”, *Mater. Des.* 119, 225–234 (2017).
- [11] M. Tokita, “Mechanism of spark plasma sintering”, in *Japanese Society of Powder Metallurgy, Kyoto*, 729–732 (2001).
- [12] H. Know, M. Lleparoux and A. Kawasaki, “Functionally graded dual-nanoparticulated-reinforced aluminium matrix bulk materials fabricated by spark plasma sintering”, *J. Mater. Sci. Technol.* 30(8), 736–742 (2014).
- [13] B.S.L. Prasad and R. Annamalai, “A study of molybdenum addition on W-Ni-Fe based heavy alloys sintered with spark plasma sintering”, *Bull. Pol. Ac.: Tech.* 67(2), 167–172 (2019).
- [14] M. Rodriguez-Reyes, M.I. Pech-Canul, J.C. Rendon-Angeles and J. Lopez-Cuevas, “Limiting the development of Al<sub>4</sub>C<sub>3</sub> to prevent degradation of Al/SiC<sub>p</sub> composites processed by pressureless infiltration”, *Compos. Sci. Technol.* 66, 1056–1062 (2006).
- [15] W. Li, H. Liang, J. Chen, S.Q. Zhu and Y.L. Chen, “Effect of SiC particles on fatigue crack growth behavior of SiC particulate – reinforced Al-Si alloy composites produced by spray forming”, *Procedia Mater. Sci.* 3, 1694–1699 (2014).
- [16] S. Nosewicz et al., “Experimental and numerical studies of micro- and macromechanical properties of modified copper-silicon carbide composites”, *Inter. J. Solids Struct.* 160, 187–200 (2019).
- [17] T. Shubert et al., “Interfacial design of Cu/SiC composites prepared by powder metallurgy for heat sink applications”, *Compos Part A-Appl. Sci. Manuf.* 38, 2398–2403 (2007).
- [18] C. Rado, B. Dreved and N. Eustathopoulos, “The role of compound formation in reactive wetting: in Cu/SiC system”, *Acta Mater.* 48, 4483–4491 (2000).
- [19] A. Brendel, C. Popescu, H. Schurmann and H. Bolt, “Interface modification of SiC-fibre/copper matrix composites by applying a titanium interlayer”, *Surf. Coat. Technol.* 200, 161–164 (2005).
- [20] S. Min, J. Blumm and A. Lindemann, “A new laser flash system for measurement of the thermophysical properties”, *Thermochim. Acta* 455, 46–49 (2007).
- [21] F. Jafari, H. Sharifi, M. Reza Seari and M. Tayebi, “Effect of reinforcement volume fraction on the wear behavior of Al-SiC composites prepared by spark plasma sintering”, *Silicon* 10, 2473–2481 (2018).
- [22] H.M. Zakaria, “Microstructural and corrosion behavior of Al/SiC metal matrix composites”, *Ain Shams Eng. J.* 5, 831–838 (2014).
- [23] K.A. Lucas and H. Clarke, *Corrosion of aluminum based metal matrix composites*, New York, John Wiley and Sons Inc., 1993.
- [24] D.M. Aylor and P.J. Moran, “Effect of reinforcement on the pitting behavior of aluminum-base metal matrix composites”, *J. Electrochem. Soc.* 132, 1277–1281 (1985).
- [25] Ch. Bombis et al., “Mechanical behaviour of nanocrystalline NaCl islands on Cu(111)”, *Phys. Rev. Lett.* 104, 185502 (2010).
- [26] H. Lin and G.S. Frankel, “Atmospheric Corrosion of Cu during constant deposition of NaCl”, *J. Electrochem. Soc.* 160, 336–344 (2013).
- [27] M. Zakaulla, A.R. Anwar Khan and P.G. Mukunda, “Effect of electroless copper coating on the corrosion behavior of aluminium based metal matrix composites reinforced with silicon carbide particles”, *J. Miner. Mater. Charact. Engin.* 2, 21–25 (2014).
- [28] N. Vasiraja and P. Nagaraj, “The effect of material gradient on the static and dynamic response of layered functionally graded material plate using finite element method”, *Bull. Pol. Ac.: Tech.* 67(4), 827–838 (2019).
- [29] M. Chmielewski et al., “Analysis of the micromechanical properties of copper-silicon carbide composites using nanoindentation measurements”, *Ceram. Inter.*, 45(7A), 9164–9173 (2019).